

DOI: 10.1002/elan.202100021

Voltammetric Determination of Neotame by Using Chitosan/Nickelnanoparticles/Multi Walled Carbon Nanotubes Biocomposite as a Modifier

Hilal İncebay*^[a] and Rumeysa Saylakci^[a]

Abstract: A selective and simple biosensor was prepared by immobilizing chitosan/nickelnanoparticles/multi-walled carbon nanotubes biocomposite on the glassy carbon electrode surface for voltammetric quantification of neotame. The properties and morphology of the modified electrode surfaces were characterized by scanning electron microscope (SEM), energy dispersive X-ray analysis (EDX). Electro oxidation of neotame on this modified surface was examined through cyclic voltammetry (CV) and square wave voltammetry (SWV) techniques. The biocomposite modified surface (Chi/NiNPs/MWCNTs/GCE) proposed in this study showed good electrocatalytic activity for neotame with an improved voltammetric peak

current at 1.004 V, unlike the bare glassy carbon electrode (GCE) surface and several other modified surfaces. Under optimum conditions, Chi/NiNPs/MWCNTs/GCE gave linear SWV responses at the range of 2 μM ~ 50 μM for neotame with 0.84 μM determination limit. This voltammetric sensor was successfully employed for the quantification of neotame on food samples and showed long-term stability, advanced voltammetric behavior, and good repeatability. Selective, accurate, and precise determination of neotame highlight the importance of this electrode in monitoring the control of food additives and ensures attract a great deal of attention.

Keywords: Carbon nanotube · chitosan · nanobiocomposite · neotame · nickel nanoparticle

1 Introduction

Neotame, a chemical dipeptide methyl ester derivative of aspartame, is an artificial sweetener approved by the U.S. Food and Drug Administration as a food additive. The sweetener does not include any neotame calories and has a sweetness factor of approximately 7,000–13,000 times greater than sucrose and 30–60 times greater than aspartame [1]. While neotame has approximately the same stability as aspartame in the acidic pH range (pH 3–5.5), neotame at neutral pH is significantly more stable than aspartame [2–4]. Dimethyl butyl (DMB), contained in the chemical structure of neotame, provides unique properties such as significantly improved sweetening power, flavor-enhancing properties, and stabilization during cooking or pasteurization [5]. The DMB group restricts the reactivity of the dipeptide amino group; therefore, no cyclization occurs unlike aspartame [6]. The absence of cyclization significantly increases neotame stability in the neutral pH compared to aspartame, hence offers possibilities for neotame in new applications that are not directly accessible for aspartame [4,7–9]. Also, the 3,3-dimethyl butyl group effectively restricts the peptidase effect on the dipeptide bond by secreting phenylalanine, which in turn reduces the production of phenylalanine and the anxiety of phenyl ketone urics [10,11].

Thanks to its low cost, high-density sweetness, safety, stability strength, and solubility, neotame has a wide potential application as a second-generation dipeptide sweetener. The acceptable daily intake of neotame has

been determined as 0–2 mg/kg body weight by the Joint Expert Committee for Food Additives and the European Food Safety Authority [12]. Because neotame has intense sweetness, it is used at a fairly low level to sweeten foods, e.g. the neotame levels in fruit juices and milk beverages are usually in the range of 2–5 and 0.5–1 mg/kg. In addition, it is important to determine the sweetener in foods very precisely and specifically, as some natural food ingredients in complex food matrices may interfere with the determination of neotame [13,14]. The information regarding the stability of neotame in food products during processing and storage is limited in the literature, so further research is needed for the safe use of quantitative information about loss or deterioration in food systems. In addition, neotame analysis is also difficult since the matrix structures of food stuff are very complex. In the reported studies, HPLC has been a widely used technique for the determination of neotame in foods [15–23]. Although methods such as HPLC and electrospray ionization mass spectrometry based on evaporative light

[a] H. İncebay, R. Saylakci
Nevsehir Hacı Bektas Veli University,
Faculty of Arts and Sciences,
Department of Molecular Biology and Genetics,
Nevsehir, Turkey
Tel: +90 384 2281000
Fax: +90 384 2153948
E-mail: hilalincebay@gmail.com

scatter detection are used to detect neotame, these are very complex, long procedures, and expensive for routine analysis. Compared to these mentioned methods, electrochemical methods have many important advantages such as selectivity, fast response time, high sensitivity, easy operation, and low cost [22,23].

Sensors can be widely used in food safety, drug delivery, medical diagnostics and health, environmental monitoring, pharmaceutical and military applications [24,25]. Electrochemical sensors are powerful analytical tools due to their advantages such as sensitivity, cost, and real-time sampling capacity [28]. Advanced and functionalized nanomaterial-based electrochemical sensors are important in many areas of analytical sciences with their fast response, sensitivity and selectivity. Nanomaterials such as gold nanoparticles, metal oxide nanoparticles, carbon nanotubes, and quantum dots are used as immobilization support for diagnostic molecules in electrochemical sensors [29]. Compared to other nanomaterials, carbon nanotubes (CNTs) have fast electron transfer capabilities, small dimensions, cylindrical shapes, large surface/volume ratio, high conductivity, and good biocompatibility. They help to increase signal sensitivity during detection with high chemical stability for signal amplification. Having superior properties such as high surface area, CNTs have been accepted as one of the most important materials for electrochemical transduction in sensors [30–33]. Besides these advantages, CNTs have been extensively studied for their mechanical, thermal, and electronic properties, as well as their interactions with molecular, ionic, or macromolecular chemical species. It is found that they are completely advantageous for the transmission of electrical signals upon recognition of the target by means of their unique structure [34] and different electronic properties [35].

Chitosan (Chi) is a natural biopolymer having properties such as biocompatibility, thin film deposition, water permeability, and high mechanical strength. It is the second most abundant biopolymer after cellulose, and suitable for forming a solid matrix in which the enzyme needs to be fixed [36]. Chitosan is compatible with both enzymes and metallic nanoparticles and can facilitate accurate enzymatic reactions and electron exchange for carbon-based materials and sensor interface [37]. Besides, considering the production and application stages of chitosan-based nanocomposite sensors, nanoparticles have adjustable size/composition and morphologies [38]. With functional properties of nanoparticle structures as such, it can significantly increase the detection ability of the modified electrode [39]. Chitosan-based sensors, which consist of nanoparticles, polymers, and hybrid composites, process fast, simple, durable, and accurate, high-precision measurements that offer exciting new opportunities for improving sensor capabilities [40–43].

In this paper, we report the determination of the neotame amount in food samples through voltammetric methods. To this end, we used a glassy carbon electrode modified with nanobiocomposite obtained from the

appropriate combination of chitosan, carbon nanotubes, and NiNPs. The modified electrode we proposed showed high sensitivity in the quantification of neotame by using square wave voltammetry. In the literature, there is a study that has used carbon nanotubes for the determination of neotame by the voltammetric method [23]. However, the procedure we developed for the electrode modification and the voltammetric technique is different from the study in question, and the sensitivity of the modified electrode we propose is higher in detecting the neotame. Experimental data showed that modifying chitosan, a natural polymer with carbon nanotubes and NiNPs, offers great electrocatalytic activity, high stability, and excellent repeatability for the oxidation of neotame. It can also be successfully applied to fruit juice samples.

2 Experimental

2.1 Materials and Reagents

All chemicals and reagents used in this study were analytically pure and commercially obtained from the relevant companies and used directly without any purification process. MWCNTs were purchased from Sigma; NaOH, and Na₂HPO₄ from Sigma-Aldrich, chloroform; and acetonitrile from VWR; NiNPs (Avr. part. size < 100 nm) KH₂PO₄ from Merck; and Chitosan, aspartame, neotame, acesulfame-K, saccharine from Sigma. All aqueous solutions were prepared using ultrapure water. In all electrochemical experiments, 0.1 M phosphate buffer solution (PBS) was used as a supporting electrolyte and was adjusted with the additions of 0.1 M NaOH and HCl to different pHs. The solutions were deprived of oxygen by passing nitrogen gas at 99 % purity before each experiment. Standard solutions were refrigerated at +4 °C for stability.

2.2 Apparatus

Gamry Interface 1000B Potentiostat /Galvanostat/Zra device was used for the electrochemical measurements. BASi Model MF-2012 glassy carbon electrode (GCE) working electrode, platinum wire (Pt wire) counter electrode, Ag/AgCl/KCl_(doy) (BASi model MF-2052) aqueous media reference electrode were used for the three-electrode cell system. OriginLab8.0 program was used to draw all the experimental data were drawn so that cross-data comparisons could be made. Thermo Orion 4 star pH meter was used for pH measurements.

2.3 Preparation of Nanocomposite Electrodes

Prior to the modifications, GCE was cleaned from the dirt on the surface and polished with 0.05 μm and 0.3 μm alumina slurries. It was then sonicated for 3 minutes in ultrapure water and acetone solutions, respectively. The cleaned electrode surface was activated at pH 3.0 at the scanning speed of 100 mV/s with cyclic voltammetry in

the potential range of -1.0 and $+1.0$ V [44]. To increase conductivity and sensitivity on the surface, MWCNTs were functionalized according to a previously reported procedure [45]. Afterwards, MWCNTs, NiNPs/MWCNTs, Chi/MWCNTs, and Chi/NiNPs/MWCNTs suspensions were prepared as follows; i) 1 mg functionalized MWCNTs, ii) 0.1 mg NiNPs with 1 mg functionalized MWCNTs; iii) 1 mg functionalized MWCNTs with 0.1 mg Chi, iv) 1 mg functionalized MWCNTs, 0.1 mg NiNPs and 0.1 mg Chi were sonicated in 5 mL chloroform for 45 minutes, respectively. $0.5 \mu\text{L}$ MWCNTs, NiNPs/MWCNTs, Chi/MWCNTs, and Chi/NiNPs/MWCNTs suspension solutions were dropped on the polished and activated GCE surface separately, and then chloroform was evaporated at room temperature (Scheme 1). MWCNTs/GCE, NiNPs/MWCNTs/GCE, Chi/MWCNTs/GCE, and Chi/NiNPs/MWCNTs/GCE modified surfaces were obtained, and neotame sensitivities were examined with cyclic voltammetry.

2.4 Optimization

MWCNTs, Chi and NiNPs were mixed with the rates of $0.5:0.5:0.5$ mg; $1.0:0.5:0.5$ mg; $1.0:0.1:0.1$ mg, respectively and the voltammetric responses for neotame were evaluated. Besides, since the amount of the Chi/NiNPs/MWCNTs suspension on the GCE surface was $1.0 \mu\text{L}$, $5.0 \mu\text{L}$, and $7.5 \mu\text{L}$, voltammetric sensitivity for neotame was investigated through cyclic voltammetry. A clearer and higher current peak formation of neotame was

observed when the mixing ratio of the Chi/NiNPs/MWCNTs suspension on the GCE surface was $1.0:0.1:0.1$ mg and the dropped suspension amount was $5.0 \mu\text{L}$.

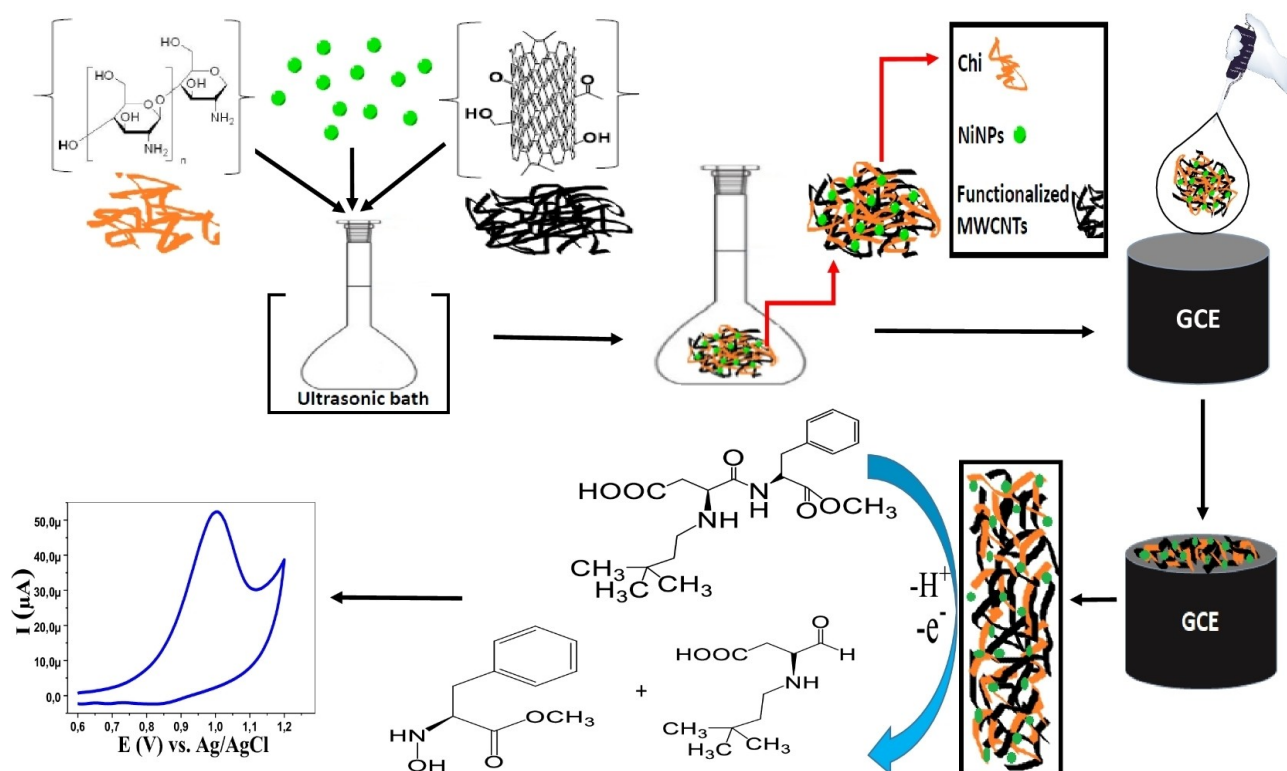
2.5 Preparation of Real Sample

Three commercial juice samples were purchased from a local store. The juice samples of 1 mL were diluted to 50 mL with 0.1 M pH 3.0 PBS. The samples were then taken into the electrochemical cell in volumes of 10 mL and SVW was used for their analysis. It was determined that the samples did not include any neotame. Therefore, prior to the dilution for recovery tests, various concentrations of neotame were added to juice samples and voltammograms were recorded.

3 Result and Discussion

3.1 Characterization of the Modified Electrode

The modifier electrode materials were characterized by SEM after immobilizing on GCE electrode surfaces. Figure 1A shows that MWCNTs are distributed homogeneously on the GCE surface since there is no aggregation on the surface. As presented in Figure 1B, chitosan exhibits a more regular layer by dispersing into the structure of MWCNTs due to its polymeric fibrous structure [46] and NiNPs are also distributed homoge-



Scheme 1. A schematic illustration of the preparation of the proposed platform.

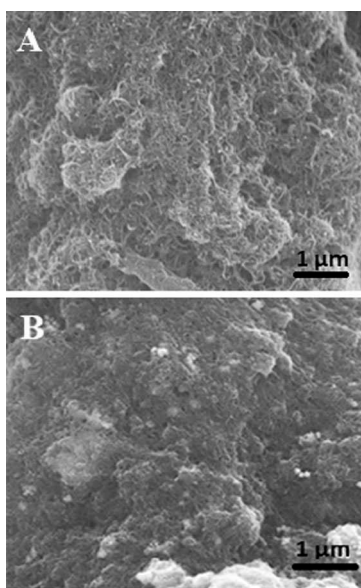


Fig. 1. SEM images of A) MWCNTs/GCE, B) Chi/NiNPs/MWCNTs/GCE.

neously within this layer. In addition, EDX results showed that the major elements in the structure of the composite forming the Chi/NiNPs/MWCNTs/GCE surface were C, O, Ni, Au (Figure 2). Here, Au was observed due to the gold coating of the electrode surface during the SEM-EDX analysis.

3.2 Electrochemical Behavior of Neo

Figure 3 presents the cyclic voltammogram of 100.0 μM neotame molecule on the surfaces of bare GCE, MWCNTs/GCE, NiNPs/MWCNTs/GCE, Chi/NiNPs/MWCNTs/GCE in 100 mM pH 3.0 PBS. No peaks of neotame were observed on the surface of bare GCE. However, the GCE surface modified with MWCNTs exhibited a wide anodic peak at 1.036 V for neotame. In addition, the voltammetric behavior of neotame was further enhanced by oxidation peaks at 1.028 V and 1.00 V, respectively on NiNPs-MWCNTs- and Chi/MWCNTs-modified GCE surface. Finally, a highly developed and well-defined anodic peak current of neotame was observed on the GCE surface modified with the Chi/NiNPs/MWCNTs bionanocomposite. Compared to the several other electrode systems developed, the Chi/NiNPs/MWCNTs/GCE surface clearly showed high electrocatalytic activity. Such a large development in the voltammetric behavior of neotame and the increase in peak current can be attributed to the appropriate combination of chitosan, NiNPs, and MWCNTs, which caused an intense increase on the active surface. This shows that chitosan, which has an abundant amino group displays a specific ability as a supportive interface for metal nanoparticles, and that the proposed platform provides an important synergistic augmentation in the electrochemical performance of neotame [47–49]. Furthermore, the lack of any observed peak in the cathodic area in the voltammetric data on all modified electrode

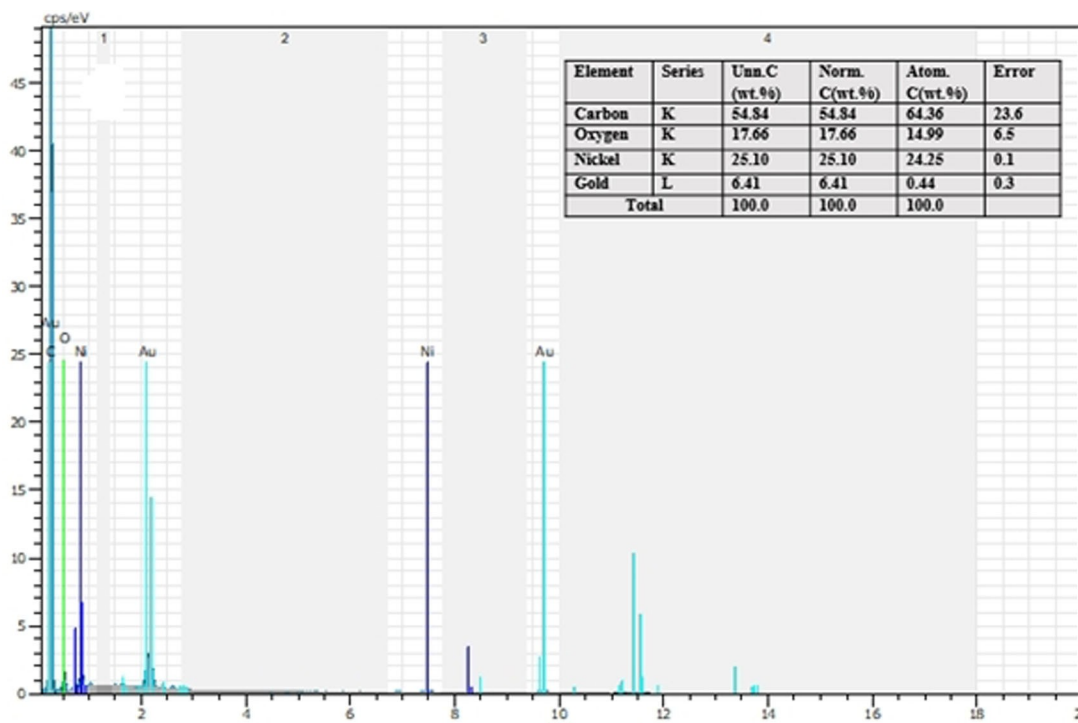


Fig. 2. C) EDX analysis of Chi/NiNPs/MWCNTs/GCE.

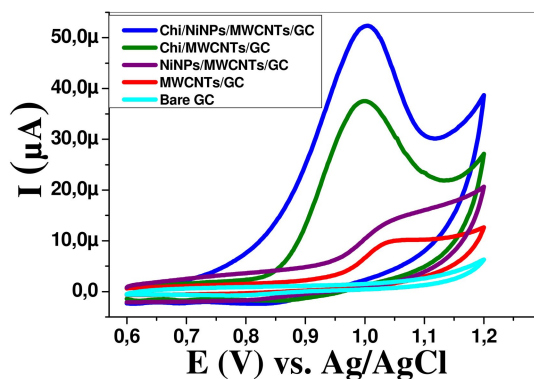


Fig. 3. CVs of 100.0 μM neotame in 0.1 M pH 3.0 PBS at Bare GCE, MWCNTs/GCE, NiNPs/MWCNTs/GCE, Chi/MWCNTs/GCE, Chi/NiNPs/MWCNTs/GCE. Scan rate: 50 mVs^{-1}

surfaces shows that neotame was exposed to irreversible oxidation.

3.3 The Effect of pH

Figure 4A shows the voltammograms regarding the oxidation of 100.0 μM neotame in the phosphate buffer in

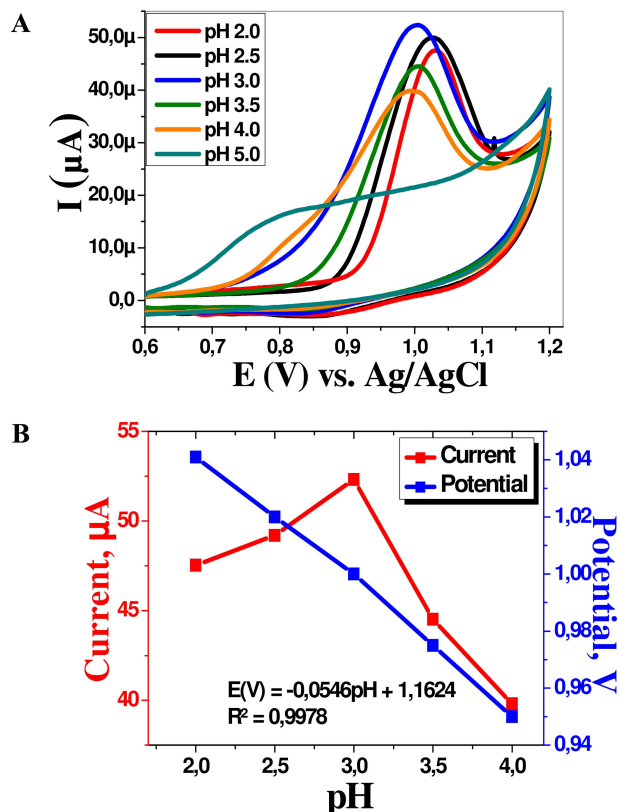


Fig. 4. A) CVs of 100.0 μM neotame at Chi/NiNPs/MWCNTs/GCE in 0.1 MPBS with pH 2.0; 2.5; 3.0; 3.5; 4.0 values. Scan rate: 50 mVs^{-1} . B) Variations of peak potential and peak current with pH.

various pHs using the Chi/NiNPs/MWCNTs/GCE surface. Accordingly, pH moved to the negative linearly with the increase in the pH values of anodic peak currents of neotame. Since the maximum peak current occurred at pH 3.0 due to the split of the amide bond into two [23,50], this value was considered optimal pH and used in all experiments with neotame. The graph of the peak potentials (E_p) and peak currents of neotame against the solution pH is presented in Figure 4B. $E(\text{V}) = -0.0546\text{pH} + 1.1624$ ($R^2 = 9978$) linear equality between the pH (2.0; 2.5; 3.0; 3.5; 4.0) and anodic peak potential of neotame were calculated and a slope of -54.6 mV/pH was obtained. Based on the following equality, Chi/NiNPs/MWCNTs/GCE surface is asserted to be the same as the number of protons and electrons in neotame oxidation, which is close to m/n value 1.

$$E_{pa} = E^0 - \frac{59 \text{ m}}{n} \text{ pH}$$

where, E_{pa} is anodic peak potential, E^0 is formal potential, m is the number of protons in the electrode reaction, and n is the number of electrons in the electrode reaction. Scheme 2 presents a possible oxidation reaction of neotame on Chi/NiNPs/MWCNTs/GCE surface.

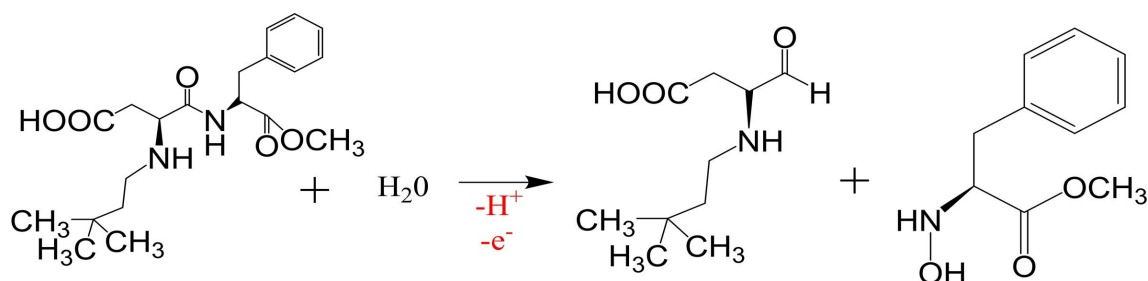
3.4 The Effect of the Scan Rate

To investigate the kinetics of the electrode reaction and determine the current type, the effect of scan rate on the oxidation of 100.0 μM neotame on the Chi/NiNPs-MWCNTs/GCE surface was examined with cyclic voltammetry between the range of $10 \sim 150 \text{ mVs}^{-1}$ as presented in Figure 5A. Here, a slight and linear shift was observed towards positive values due to the changes in the surface layer on the oxidation of neotame at the increasing scan rates of the peak current. If the correlation coefficient of the $v^{1/2}$ - I graph is in the range of 0.75–1.0 and the slope of $\log v$ - $\log I$ graph is around 0.5 [51], the current is regarded diffusion-controlled [52]. Considering this, the correlation coefficient (R^2) of the $v^{1/2}$ - I graph presented in Figure 5B was 0.9995 and the slope of the graph presented in Figure 5C was 0.6994, which indicates that the current was realized by a diffusion-controlled process. In addition, the Laviron equation presented below was used to determine the number of electrons involved in the oxidation of neotame.

$$E_{pa} = E^0 + 2.303 \left(\frac{RT}{\alpha nF} \right) \log \left(\frac{RTk^0}{\alpha nF} \right) + 2.303 \left(\frac{RT}{\alpha nF} \right) \log v$$

where, E_{pa} is anodic peak potential, E^0 is standard cell potential, α is electron transfer coefficient, k^0 is standard heterogeneous speed constant, and n is the number of electrons transferred.

The slope of the graph regarding the E_{pa} of neotame against the $\log v$ (Figure 5D) was calculated as 0.0675. The



Scheme 2. Possible oxidation mechanism of neotame at Chi/NiNPs/MWCNTs/GCE.

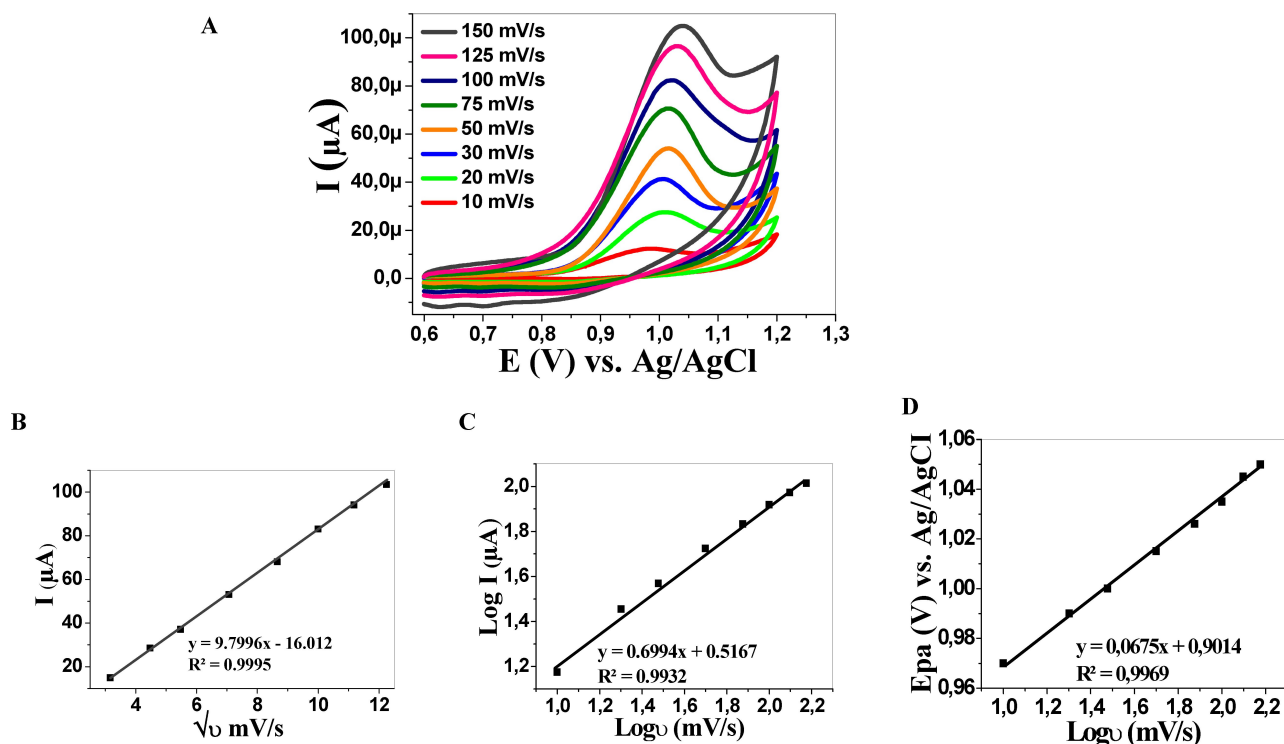


Fig. 5. A) CVs of 100.0 μM neotame in 0.1 M PBS (pH 3.0) at Chi/NiNPs/MWCNTs/GCE. Scan rates from 10 $mV s^{-1}$ to 150 $mV s^{-1}$. A plot of B) peak current versus square root scan rate, C) logarithm of anodic peak currents of neotame versus logarithm of scan rates, D) anodic peak potentials of neotame versus logarithm of scan rates

electron transfer coefficient for an irreversible reaction, α is known to be approximately 0.5 [53]. In this case, the results showed that the neotame went through an oxidation process with a single electron transfer (Scheme 2).

3.5 Analytical Performance

Under optimized conditions, SWV was used to determine neotame at a higher precision on the Chi/NiNPs/MWCNTs/GCE surface. For this purpose, SWV voltammograms obtained at different concentrations of neotame are presented in Figure 6A. The calibration graph formed by the SWV voltammograms is presented in Figure 6B. The obtained results showed that the neotame with the equation of $I_{pa}(\mu A) = 0.5415 C(\mu M) + 5.5455$ gives a line-

ar graph between the range of 2–50 μM with a correlation coefficient of 0.5455. The determination limit (LOD) was calculated as 0.84 μM (3.3(Sb/m)) and the quantification limit (LOQ) as 2.56 (10(Sb/m)). Table 1 shows the analytical parameters of a number of electrodes reported in the literature for the determination of neotame by the voltammetric method. When the voltammetric platforms reported in this studies and the voltammetric platform proposed in the present study are compared, we can say that we prepared a very precise electrode surface in determining the neotame Table 1. Besides, Joint FAO-WHO Expert Committee Report on Food Additives (JECFA) identified the daily consumption of neotame as 2 mg/kg body weight/day. Compared to this value, the amount of neotame that can be determined on the platform we proposed is lower.

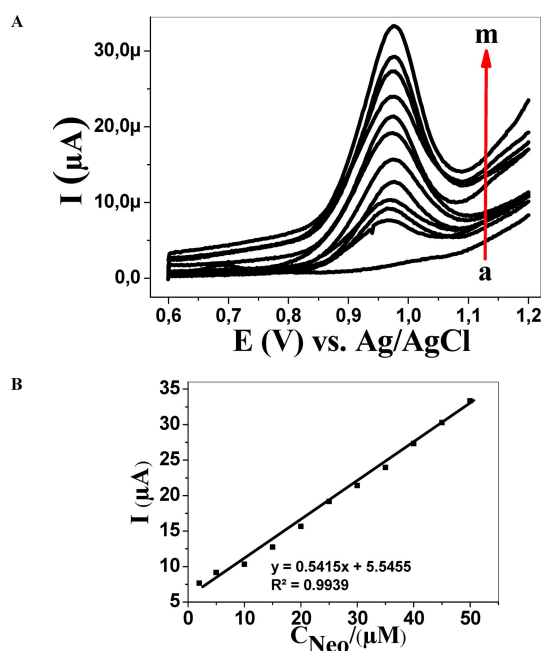


Fig. 6. A) SWVs of various concentrations of neotame at Chi/NiNPs/MWCNTs/GCE in 0.1 MPBS at pH 3.0. Neotame concentrations: 0.0 μM ; 2.0 μM ; 5.0 μM ; 10.0 μM ; 15.0 μM ; 20.0 μM ; 25.0 μM ; 30.0 μM ; 35.0 μM ; 40.0 μM ; 45.0 μM ; 50.0 μM . Frequency: 22 Hz. Step potential: 100 mV/s. Amplitude: 50 mV/s. B) A plot of peak currents versus the concentrations of neotame.

3.6 Reproducibility, Repeatability, Stability, and Selectivity

Reproducibility, repeatability stability, and selectivity are the main factors in determining the proposed sensor performance. To this end, 4 different electrodes were prepared in the same way for reproducibility and compared the voltammograms using CV. For repeatability, the same electrode was prepared each time and cyclic voltammograms were taken 5 times and compared to each other. For the measurement of 100.0 μM neotame with 5 repetitions, the relative standard deviation (RSD) values of the reproducibility and the repeatability of the Chi/NiNPs/MWCNTs/GCE surface were calculated as 1.18 % and 1.03 %, respectively (Figure 7A). This showed that the Chi/NiNPs/MWCNTs/GCE surface has very good reproducibility and repeatability with very low % RSD values. In addition, for the long-term stability of the

developed sensor, the Chi/NiNPs/MWCNTs/GC electrode was incubated in pH 3.0 PBS for 4 weeks. The cyclic voltammograms of the incubated electrodes were recorded with certain periods and compared to the voltammograms prior to the incubation as presented in Figure 7B. The change in the peak current of neotame was only 5.7 %. This slight decline in peak current showed that Chi/NiNPs/MWCNTs/GCE has good stability. The selectivity of the proposed new electrode towards neotame was investigated in the presence of possible types of interference with 100 times higher concentration than neotame. For this purpose, interferences such as saccharine, aspartame, acesulfame-K were prepared by adding to the solutions containing 20 μM , 50 μM and 100 μM neotame at pH 3.0 PBS, and cyclic voltammograms recorded under optimum conditions were given in Figure 7C. It can be seen that there is a regular increase in peak currents of the increased neotame concentrations. In addition, voltammograms of 100.0 μM neotame solutions that contain and do not contain interferences having 100 times higher concentrations were recorded in pH 3.0 PBS and compared with each other (Figure 7D). It was clear that none of the interference species made any changes (a decrease of 2.75 %) in the voltammetric signal response of neotame. Furthermore, experimental results showed that the interference species has no significant impact on the peak shape potential and current of neotame, and the proposed sensor has a high selectiveness.

3.7 Analysis of Real Samples

The applicability of the developed sensor was examined by applying SWV to fruit juice samples under optimum conditions. Initially, no neotame was detected in the juice samples. For this reason, neotame was added to the juice samples in different concentrations using the standard addition method, and the square wave voltammetric quantification of the neotame in fruit juice samples was directed to the calibration plot. Each concentration of samples was tested with 5 repetitions as summarized in Table 2. Good recoveries between 93.52 % and 102.32 % for the proposed electrode, minor errors between -3.10 and $+3.10$, and RSD values between 1.03 % and 3.92 % were obtained. These results showed that Chi/NiNPs/MWCNTs/GCE surface has a high sensitivity, good confidence, and great potential in detecting neotame,

Table 1. Comparison of the analytical performance of the proposed sensor for neotame detection with other electrodes from the literature.

Electrode configuration	Method	Linear range/ μM	Detection limit/ μM	Ref.
CuNPs-APDC-MWCNTs- β -CD/GCE	DPV	30–200	13	[23]
CaE/AuNPs/MWCNTs/GCE	DPV	1120–3340	27	[54]
Chi/NiNPs/MWCNTs/GCE	SWV	2–50	0.84	This work

Multiwalled carbon nanotubes (MWCNTs); gold nanoparticles (AuNPs); carboxyl esterase enzyme (CaE); differential pulse voltammetry (DPV); coppernanoparticles (CuNPs); ammonium piperidine dithiocarbamate (APDC); β -cyclodextrin (β -CD); nickel nanoparticles (NiNPs); Chitosan (Chi).

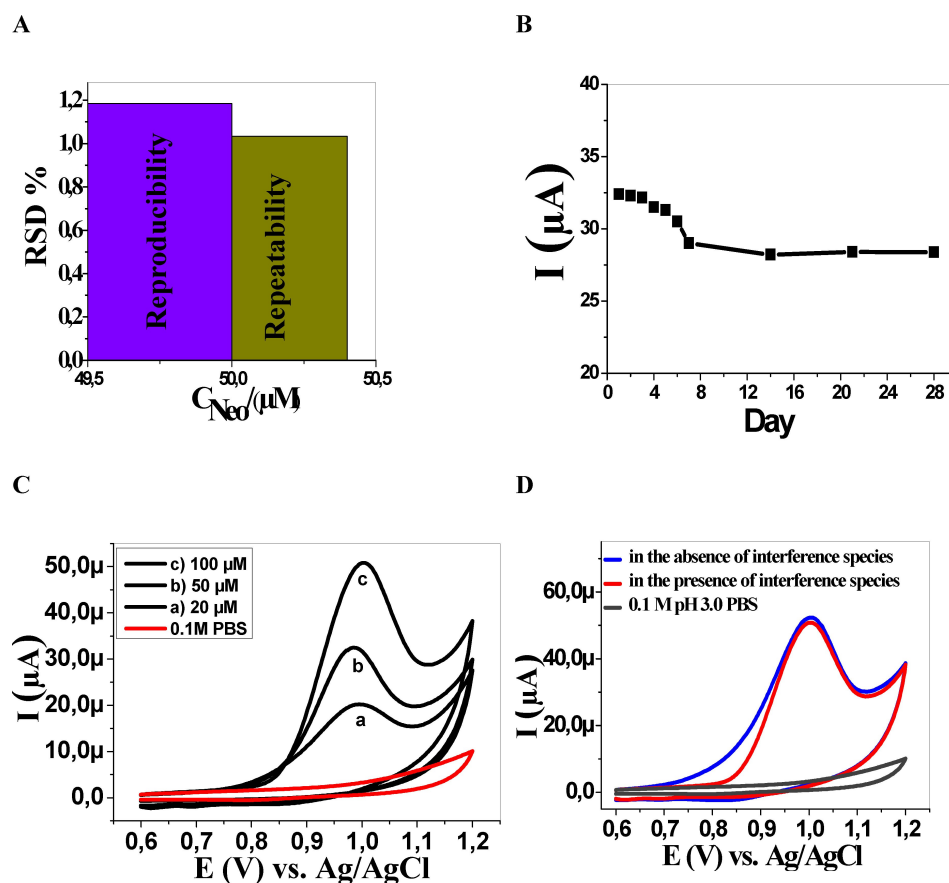


Fig. 7. A) RSD% of reproducibility and repeatability B) stability C) CVs of 20 μM , 50 μM and 100 μM of neotame in the presence of interference species D) CVs of 100 μM neotame in the presence of interference species and in the absence of interference species in pH 3.0 PBS of proposed electrode.

Table 2. Recovery, found, relative standard deviations (RSD) results of neotame added to real samples.

Samples	Added(μM)	Found (μM)	Peak current(μA)	RSD (%)	Recovery(%)	Error (%)
Sample-I	0	Not detected	–	–	–	–
	2	1.96	6.66	2.56	98.19	-1.80
	4	4.05	8.15	1.03	101.34	+1.34
	8	7.98	10.95	3.92	99.76	-0.23
Sample-II	0	Not detected	–	–	–	–
	2	1.93	5.86	1.31	96.89	+3.10
	4	4.09	7.25	1.4	102.32	+2.32
	8	7.96	9.75	1.27	99.61	+0.38
Sample-III	0	Not detected	–	–	–	–
	2	1.87	7.9	2.19	93.52	-3.10
	4	4.05	9.35	1.09	101.44	+2.32
	8	7.98	11.95	2.30	99.75	-0.38

$n=5$ RSD (%) = (Standard deviation/The average of the data obtained by repeating 5 times.) $\times 100$. Error (%) = [(found value – added value)/added value] $\times 100$.

which is food additives in real food samples, by the voltammetric method.

4 Conclusion

A nanobiocomposite was prepared by decorating chitosan, which a natural biopolymer, with carbon nanotubes

and NiNPs. It was found that this nanobiocomposite could be used as a suitable modifier in the voltammetric method for the quantification of neotame. Compared to the other electrodes prepared, the Chi/NiNPs/MWCNTs/GCE electrode surface offered a better electrocatalyst activity with a well-defined peak at 1.0 V for the oxidation of neotame. Excellent linearity was achieved between the concentra-

tions of neotame in the range of 2 μM –50 μM and the anodic peak currents. The proposed voltammetric platform was able to determine the neotame with a determination limit of 0.84 μM , which is much lower than the voltammetric platforms previously reported in the literature (Table 1). This nanobiostructured electrode showed quite high precision, good repeatability, excellent accuracy, and good stability, which indicated that neotame can be used successfully in determining fruit juice samples. Considering that neotame is commonly used in some countries while it is banned in many others due to its harmful effects, the capability of the proposed platform to determine very low amounts of neotame is very important.

Acknowledgment

We would like to thank Nevşehir Hacı Bektaş Veli University Research Foundation, which provided financial support for this research under the 162F20 project.

Data Availability Statement

Encourages Data Sharing-Data available on request from the authors

References

- [1] C. Shwide-Slavin, C. Swift, T. Ross, *Diabetes Spectr.* **2012**, 25, 104–110, <https://doi.org/10.2337/diaspect.25.2.104>.
- [2] C. Nofre, J. M. Tinti, *Food Chem.* **2000**, 69, 245–257, [https://doi.org/10.1016/S0308-8146\(99\)00254-X](https://doi.org/10.1016/S0308-8146(99)00254-X).
- [3] L. Zhu, G. Wang, B. Dong, C. C. Peng, Y. Y. Tian, L. M. Gong, *Anim. Feed Sci. Technol.* **2016**, 214, 86–94, <https://doi.org/10.1016/j.anifeedsci.2016.02.013>.
- [4] A. Kumari, S. Arora, S. Choudhary, A. K. Singh, S. K. Tomar, *Int. J. Dairy Technol.* **2018**, 71, 81–88, <https://doi.org/10.1111/1471-0307.12381>.
- [5] A. Kumari, S. Arora, A. K. Singh, S. Choudhary, *LWT-Food Sci. Technol.* **2016**, 70, 142–147, <https://doi.org/10.1016/j.lwt.2016.02.045>.
- [6] S. Arora, H. Gawande, V. S. Balbir Kaur Wadhwa, V. George, G. S. Sharma, A. K. Singh, *Int. J. Dairy Technol.* **2010**, 63, 127–135, <https://doi.org/10.1111/j.1471-0307.2009.00555>.
- [7] A. Kumari, S. Choudhary, S. Arora, V. Sharma, *Food Chem.* **2016**, 196, 533–538, <https://doi.org/10.1016/j.foodchem.2015.09.082>.
- [8] D. Yang, B. Chen, *Food Addit. Contam. - Part A Chem. Anal. Control. Expo. Risk Assess.* **2010**, 27, 1221–1225, <https://doi.org/10.1080/19440049.2010.487875>.
- [9] H. M. Gawande, S. Arora, V. Sharma, B. K. Wadhwa, *J. Food Sci. Technol.* **2015**, 52, 2373–2379, <https://doi.org/10.1007/s13197-013-1206-5>.
- [10] *Food Additives Permitted For Direct Addition To Food For Human Consumption*, in: *CRC Master Keyword Guid.* Food, **2003**, <https://doi.org/10.1201/9780203504529.chb6>.
- [11] S. Olivier-Van Stichelen, K. I. Rother, J. A. Hanover, *Glycobiology* **2017**, 10, 1360, <https://doi.org/https://doi.org/10.1093/glycob/cwx086>.
- [12] *EFSA J.* **2013**, 11, 3301, <https://doi.org/10.2903/j.efsa.2013.3301>.
- [13] D. Yang, B. Chen, *Food Addit. Contam.*, **2010**, 27, 1221–1225, <https://doi.org/10.1080/19440049.2010.487875>.
- [14] M. Sha, Z. Zhang, J. Liu, H. Wang, *Anal. Lett.* **2017**, 50, 936–944, <https://doi.org/10.1080/00032719.2016.1205079>.
- [15] M. G. Kokotou, N. S. Thomaidis, *Anal. Lett.* **2018**, 51, 49–72, <https://doi.org/10.1080/00032719.2017.1326124>.
- [16] D. de Queiroz Pane, C. B. Dias, A. D. Meinhart, C. A. Ballus, H. T. Godoy, *J. Food Sci. Technol.* **2015**, 52, 6900–6913, <https://doi.org/10.1007/s13197-015-1816-1>.
- [17] P. Kubica, J. Namiesnik, A. Wasik, *Anal. Bioanal. Chem.* **2015**, 407, 1505–1512, <https://doi.org/10.1007/s00216-014-8355-x>.
- [18] M. Sha, Z. Zhang, J. Liu, H. Wang, *Anal. Lett.* **2017**, 50, 936–944, <https://doi.org/10.1080/00032719.2016.1205079>.
- [19] J. Tang, L. Yuan, Y. Xiao, X. Wang, S. Wang, *Chinese J. Chromatogr. (Se Pu)*. **2019**, 37, 619–625, <https://doi.org/10.3724/SP.J.1123.2019.01012>.
- [20] Y. G. Zhao, M. Q. Cai, X. H. Chen, S. D. Pan, S. S. Yao, M. C. Jin, *Food Res. Int.* **2013**, 52, 350–358, <https://doi.org/10.1016/j.foodres.2013.03.038>.
- [21] H. S. Lim, S. K. Park, I. S. Kwak, H. Il Kim, J. H. Sung, S. J. Jang, M. Y. Byun, S. H. Kim, *Food Sci. Biotechnol.* **2013**, 22, 233–240, <https://doi.org/10.1007/s10068-013-0072-2>.
- [22] E. Gvozdić, I. Matic Bujagić, T. Đurkić, S. Grujić, *Microchem. J.* **2020**, <https://doi.org/10.1016/j.microc.2020.105071>.
- [23] A. Bathinapatla, S. Kanchi, P. Singh, M. I. Sabela, K. Bisetty, *Biosens. Bioelectron.* **2015**, 67, 200–207, <https://doi.org/10.1016/j.bios.2014.08.017>.
- [24] A. V. T. Le, Y. L. Su, S. H. Cheng, *Electrochim. Acta.* **2019**, 300, 67–76, <https://doi.org/10.1016/j.electacta.2019.01.020>.
- [25] L. Yu, H. Zheng, M. Shi, S. Jing, L. Qu, *Food Anal. Methods.* **2017**, 10, 200–209, <https://doi.org/10.1007/s12161-016-0569-4>.
- [26] G. Maduraiveeran, M. Sasidharan, V. Ganesan, *Biosens. Bioelectron.* **2018**, 103, 113–129, <https://doi.org/10.1016/j.bios.2017.12.031>.
- [27] R. C. Pangule, S. J. Brooks, C. Z. Dinu, S. S. Bale, S. L. Salmon, G. Zhu, D. W. Metzger, R. S. Kane, J. S. Dordick, *ACS Nano.* **2010**, 4, 3993–4000, <https://doi.org/10.1021/nn100932t>.
- [28] D. Grieshaber, R. MacKenzie, J. Vörös, E. Reimhult, *Sensors.* **2008**, 8, 1400–1458, <https://doi.org/10.3390/s8031400>.
- [29] M. Holzinger, A. Le Goff, S. Cosnier, *Front. Chem.* **2014**, 2, 63, <https://doi.org/10.3389/fchem.2014.00063>.
- [30] R. V. Mundra, X. Wu, J. Sauer, J. S. Dordick, R. S. Kane, *Curr. Opin. Biotechnol.* **2014**, 28, 25–37, <https://doi.org/10.1016/j.copbio.2013.10.012>.
- [31] V. Rastogi, P. Yadav, S. S. Bhattacharya, A. K. Mishra, N. Verma, A. Verma, J. K. Pandit, *J. Drug Deliv.* **2014**, 23, <https://doi.org/10.1155/2014/670815>.
- [32] H. Zhang, L. Hou, X. Jiao, Y. Ji, X. Zhu, H. Li, X. Chen, J. Ren, Y. Xia, Z. Zhang, *Curr. Pharm. Biotechnol.* **2014**, 14, 1105–1117, <https://doi.org/10.2174/1389201015666140408123710>.
- [33] M. Adeli, R. Soleyman, Z. Beiranvand, F. Madani, *Chem. Soc. Rev.* **2013**, 42, 5231–5256, <https://doi.org/10.1039/c3cs35431h>.
- [34] Q. Zhao, Z. Gan, Q. Zhuang, *Electroanalysis.* **2002**, 14, 1609–1613, <https://doi.org/10.1002/elan.200290000>.
- [35] C. M. Tilmaci, M. C. Morris, *Front. Chem.* **2015**, 3, 59, <https://doi.org/10.3389/fchem.2015.00059>.
- [36] I. M. Apetrei, C. Apetrei, *Sensors (Switzerland)*. **2016**, 16, 422, <https://doi.org/10.3390/s16040422>.

- [37] E. Muthusankar, D. Ragupathy, *Sens. Lett.* **2018**, *16*, 81–91, <https://doi.org/10.1166/sl.2018.3925>.
- [38] P. Narasimman, M. Pushpavanam, V. M. Periasamy, *Synthesis, Appl. Surf. Sci.* **2011**, *258*, 590–598, <https://doi.org/10.1016/j.apsusc.2011.08.038>.
- [39] C. Y. Huang, J. H. Lai, *Org. Electron.* **2016**, *32*, 244–249, <https://doi.org/10.1016/j.orgel.2016.02.031>.
- [40] M. A. Kafi, A. Paul, R. Dahiya, *Graphene oxide-chitosan based flexible biosensor*, in: *Proc. IEEE Sensors*, **2017**, 1–3, <https://doi.org/10.1109/ICSENS.2017.8234441>.
- [41] I. M. Apetrei, C. Apetrei, *Materials (Basel)*. **2019**, *12*, 1009, <https://doi.org/10.3390/ma12071009>.
- [42] A. Vilouras, A. Paul, M. A. Kafi, R. Dahiya, *IEEE Sens. J.*, **2018**, *20*, 13, <https://doi.org/10.1109/ICSENS.2018.8589730>.
- [43] P. Gomathi, H. Do Ghim, D. Ragupathy, *Macromol. Res.* **2011**, *19*, 442, <https://doi.org/10.1007/s13233-011-0515-7>.
- [44] A. K. Baytak, T. Teker, S. Duzmen, M. Aslanoglu, *Mater. Sci. Eng. C*. **2016**, *1*, 125–131, <https://doi.org/10.1016/j.msec.2016.05.008>.
- [45] A. K. Baytak, M. Aslanoglu, *J. Electroanal. Chem.* **2015**, *757*, 210–215, <https://doi.org/10.1016/j.jelechem.2015.09.041>.
- [46] K. Kalantari, A. M. Afifi, H. Jahangirian, T. J. Webster, *Carbohydr. Polym.* **2019**, *1*, 588–600, <https://doi.org/10.1016/j.carbpol.2018.12.011>.
- [47] M. Hosseini Ghalehno, M. Mirzaei, M. Torkzadeh-Mahani, *Bioelectrochemistry* **2019**, *130*, <https://doi.org/10.1016/j.bioelechem.2019.06.007>.
- [48] M. Figiela, M. Wysokowski, M. Galinski, T. Jesionowski, I. Stepniak, *Sens. Actuators B* **2018**, *272*, 296–307, <https://doi.org/10.1016/j.snb.2018.05.173>.
- [49] M. B. Gholivand, L. Mohammadi-Behzad, H. Hosseinkhani, *Anal. Biochem.* **2016**, *493*, 35–43, <https://doi.org/10.1016/j.jab.2015.08.033>.
- [50] R. A. Medeiros, A. E. de Carvalho, R. C. Rocha-Filho, O. Fatibello-Filho, *Talanta*. **2008**, *76*, 685–689, <https://doi.org/10.1016/j.talanta.2008.04.015>.
- [51] Y. Lin, K. Liu, C. Liu, L. Yin, Q. Kang, L. Li, B. Li, *Electrochim. Acta* **2014**, *133*, 492–500, <https://doi.org/10.1016/j.jelectacta.2014.04.095>.
- [52] J. Li, D. Kuang, Y. Feng, F. Zhang, M. Liu, *Microchim. Acta*. **2011**, *172*, 379–386, <https://doi.org/10.1007/s00604-010-0512-0>.
- [53] E. O. Barnes, X. Chen, P. Li, R. G. Compton, *J. Electroanal. Chem.* **2014**, *720–721*, 92–100, <https://doi.org/10.1016/j.jelechem.2014.03.028>.
- [54] M. Lephala, S. Kanchi, M. I. Sabela, K. Bisetty, *Electroanalysis* **2020**, *32*, 2669–2680. <https://doi.org/10.1002/elan.202060208>.

Received: February 16, 2021

Accepted: March 1, 2021

Published online on March 9, 2021